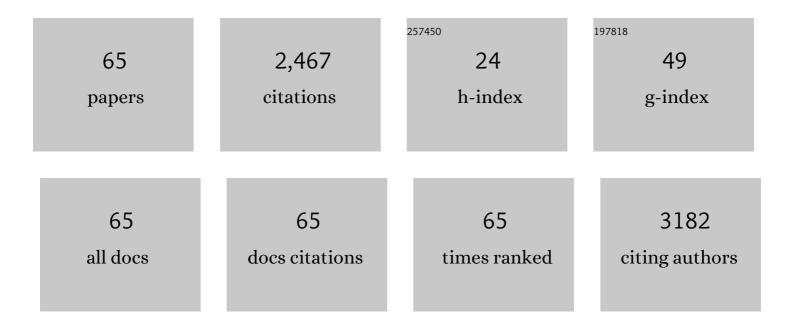


## List of Publications by Year in descending order

Source: https://exaly.com/author-pdf/5625635/publications.pdf Version: 2024-02-01



VAO VAO

#	Article	IF	CITATIONS
1	Enhanced sensitivity of ammonia sensor using graphene/polyaniline nanocomposite. Sensors and Actuators B: Chemical, 2013, 178, 485-493.	7.8	425
2	Graphene oxide thin film coated quartz crystal microbalance for humidity detection. Applied Surface Science, 2011, 257, 7778-7782.	6.1	204
3	Humidity sensing behaviors of graphene oxide-silicon bi-layer flexible structure. Sensors and Actuators B: Chemical, 2012, 161, 1053-1058.	7.8	167
4	The effect of ambient humidity on the electrical properties of graphene oxide films. Nanoscale Research Letters, 2012, 7, 363.	5.7	151
5	Room-temperature highly sensitive CO gas sensor based on Ag-loaded zinc oxide/molybdenum disulfide ternary nanocomposite and its sensing properties. Sensors and Actuators B: Chemical, 2017, 253, 1120-1128.	7.8	140
6	Application of the Variational-Mode Decomposition for Seismic Time–frequency Analysis. IEEE Journal of Selected Topics in Applied Earth Observations and Remote Sensing, 2016, 9, 3821-3831.	4.9	97
7	Room Temperature Methane Sensor Based on Graphene Nanosheets/Polyaniline Nanocomposite Thin Film. IEEE Sensors Journal, 2013, 13, 777-782.	4.7	92
8	Novel QCM humidity sensors using stacked black phosphorus nanosheets as sensing film. Sensors and Actuators B: Chemical, 2017, 244, 259-264.	7.8	82
9	Fabrication of platinum-loaded cobalt oxide/molybdenum disulfide nanocomposite toward methane gas sensing at low temperature. Sensors and Actuators B: Chemical, 2017, 252, 624-632.	7.8	82
10	Facile fabrication of high sensitivity cellulose nanocrystals based QCM humidity sensors with asymmetric electrode structure. Sensors and Actuators B: Chemical, 2020, 302, 127192.	7.8	76
11	Investigation of the stability of QCM humidity sensor using graphene oxide as sensing films. Sensors and Actuators B: Chemical, 2014, 191, 779-783.	7.8	66
12	Impedance analysis of quartz crystal microbalance humidity sensors based on nanodiamond/graphene oxide nanocomposite film. Sensors and Actuators B: Chemical, 2015, 211, 52-58.	7.8	61
13	Multi-Walled Carbon Nanotubes/Graphene Oxide Composites for Humidity Sensing. IEEE Sensors Journal, 2013, 13, 4749-4756.	4.7	56
14	Bandwidth Extension of Doherty Power Amplifier Using Complex Combining Load With Noninfinity Peaking Impedance. IEEE Transactions on Microwave Theory and Techniques, 2019, 67, 765-777.	4.6	52
15	High-stability quartz crystal microbalance ammonia sensor utilizing graphene oxide isolation layer. Sensors and Actuators B: Chemical, 2014, 196, 183-188.	7.8	45
16	Quartz Crystal Microbalance Humidity Sensors Based on Nanodiamond Sensing Films. IEEE Nanotechnology Magazine, 2014, 13, 386-393.	2.0	45
17	Hierarchically MoS2 nanospheres assembled from nanosheets for superior CO gas-sensing properties. Materials Research Bulletin, 2018, 101, 132-139.	5.2	41
18	Fabrication of miniaturized CSRR-loaded HMSIW humidity sensors with high sensitivity and ultra-low humidity hysteresis. Sensors and Actuators B: Chemical, 2018, 256, 1100-1106.	7.8	39

ΥΑΟ ΥΑΟ

#	Article	IF	CITATIONS
19	Development of a highly sensitive humidity sensor based on the capacitive micromachined ultrasonic transducer. Sensors and Actuators B: Chemical, 2019, 286, 39-45.	7.8	31
20	SIW resonator humidity sensor based on layered black phosphorus. Electronics Letters, 2017, 53, 249-251.	1.0	30
21	A facile method to graphene oxide/polyaniline nanocomposite with sandwich-like structure for enhanced electrical properties of humidity detection. Analytica Chimica Acta, 2019, 1080, 178-188.	5.4	29
22	High Sensitivity and High Stability QCM Humidity Sensors Based on Polydopamine Coated Cellulose Nanocrystals/Graphene Oxide Nanocomposite. Nanomaterials, 2020, 10, 2210.	4.1	28
23	Humidity-Sensing Properties of a BiOCl-Coated Quartz Crystal Microbalance. ACS Omega, 2020, 5, 18818-18825.	3.5	25
24	Acetylene Gas-Sensing Properties of Layer-by-Layer Self-Assembled Ag-Decorated Tin Dioxide/Graphene Nanocomposite Film. Nanomaterials, 2017, 7, 278.	4.1	24
25	A Precise Harmonic Control Technique for High Efficiency Concurrent Dual-Band Continuous Class-F Power Amplifier. IEEE Access, 2018, 6, 51864-51874.	4.2	24
26	Detection of ethanol and methanol vapors using polymer-coated piezoresistive Si bridge. Sensors and Actuators B: Chemical, 2011, 155, 519-523.	7.8	23
27	Highly sensitive CMUT-based humidity sensors built with nitride-to-oxide wafer bonding technology. Sensors and Actuators B: Chemical, 2019, 294, 123-131.	7.8	23
28	Influence of the oxygen content on the humidity sensing properties of functionalized graphene films based on bulk acoustic wave humidity sensors. Sensors and Actuators B: Chemical, 2016, 222, 755-762.	7.8	22
29	Design of High Efficiency Broadband Continuous Class-F Power Amplifier Using Real Frequency Technique With Finite Transmission Zero. IEEE Access, 2018, 6, 61983-61993.	4.2	22
30	Simulation analysis and experimental verification for sensitivity of IDE-QCM humidity sensors. Sensors and Actuators B: Chemical, 2021, 341, 129992.	7.8	22
31	Self-Assembly of Polyelectrolytic/Graphene Oxide Multilayer Thin Films on Quartz Crystal Microbalance for Humidity Detection. IEEE Sensors Journal, 2014, 14, 4078-4084.	4.7	20
32	Design of Concurrent Dual-Band Continuous Class-J Mode Doherty Power Amplifier With Precise Impedance Terminations. IEEE Microwave and Wireless Components Letters, 2019, 29, 348-350.	3.2	19
33	Assessing the Mass Sensitivity for Different Electrode Materials Commonly Used in Quartz Crystal Microbalances (QCMs). Sensors, 2019, 19, 3968.	3.8	18
34	Development of a Novel CMUT-Based Concentric Dual-Element Ultrasonic Transducer: Design, Fabrication, and Characterization. Journal of Microelectromechanical Systems, 2018, 27, 538-546.	2.5	16
35	Novel Quartz Crystal Capacitive Sensor for Micro Displacement Detection. IEEE Sensors Journal, 2012, 12, 2145-2149.	4.7	15
36	Does mode mixing matter in EMD-based highlight volume methods for hydrocarbon detection? Experimental evidence. Journal of Applied Geophysics, 2016, 132, 193-210.	2.1	15

ΥΑΟ ΥΑΟ

#	Article	IF	CITATIONS
37	Fabrication and Characterization of Highly Sensitive Acetone Chemical Sensor Based on ZnO Nanoballs. Materials, 2017, 10, 799.	2.9	15
38	Ringed Electrode Configuration Enhances the Sensitivity of QCM Humidity Sensor Based on Lignin Through Fringing Field Effect. IEEE Sensors Journal, 2021, 21, 22450-22458.	4.7	15
39	Effect of humidity on electrical properties of micro/nano-polyaniline thin films with different D-CSA doping degree. Measurement: Journal of the International Measurement Confederation, 2013, 46, 411-419.	5.0	13
40	Seismic attenuation estimation using a complete ensemble empirical mode decomposition-based method. Marine and Petroleum Geology, 2016, 71, 296-309.	3.3	11
41	High Sensitivity of Ammonia Sensor through 2D Black Phosphorus/Polyaniline Nanocomposite. Nanomaterials, 2021, 11, 3026.	4.1	11
42	Effect of p-Type Buried Layer Dose on Hot Carrier Degradation of RONin 700 V Triple RESURF nLDMOS. IEEE Electron Device Letters, 2016, 37, 242-244.	3.9	9
43	Waveletâ€based cepstrum decomposition of seismic data and its application in hydrocarbon detection. Geophysical Prospecting, 2016, 64, 1441-1453.	1.9	9
44	Analysis of the Effect of Electrode Materials on the Sensitivity of Quartz Crystal Microbalance. Nanomaterials, 2022, 12, 975.	4.1	8
45	Enhanced sensitivity of quartz crystal proximity sensors using an asymmetrical electrodes configuration. Sensors and Actuators A: Physical, 2017, 258, 95-100.	4.1	7
46	Performance Enhancement of Interdigital Electrode-Piezoelectric Quartz Crystal (IDE-PQC) Salt Concentration Sensor by Increasing the Electrode Area of Piezoelectric Quartz Crystal (PQC). Sensors, 2018, 18, 3224.	3.8	7
47	Optimized Dynamic \$ext{R}_{ mathrm{scriptscriptstyle ON}}\$ With p-Type Buried Layer Bridge in 700-V Triple RESURF nLDMOS. IEEE Transactions on Electron Devices, 2017, 64, 3287-3292.	3.0	5
48	Crossâ€sensitivity reduction of QCM humidity sensor using graphene oxide membrane as filter layer. Electronics Letters, 2014, 50, 1447-1449.	1.0	4
49	A 0.18- <inline-formula> <tex-math notation="LaTeX">\$mu\$ </tex-math> </inline-formula> m LDMOS With Excellent Ronsp and Uniformity by Optimized Manufacture Process. IEEE Transactions on Semiconductor Manufacturing, 2019, 32, 129-133.	1.7	4
50	Sensitivity Enhancement of Quartz Crystal Capacitive Sensor Using Series Inductive Reactance. IEEE Sensors Journal, 2014, 14, 2012-2018.	4.7	3
51	An Accurate Three-Input Nonlinear Model for Joint Compensation of Frequency-Dependent I/Q Imbalance and Power Amplifier Distortion. IEEE Access, 2019, 7, 140651-140664.	4.2	3
52	A High-Q Quartz Crystal Microbalance with Mass Sensitivity up to 1017 Hz/kg. Chinese Physics Letters, 2019, 36, 120702.	3.3	3
53	Fundamental resonance frequency dependence of the proximity effect of quartz crystal resonators. Japanese Journal of Applied Physics, 2015, 54, 116701.	1.5	2

ΥΑΟ ΥΑΟ

#	Article	IF	CITATIONS
55	A 500-V High ON-BV Parasitic JFET With an Optimized Drift Region. IEEE Transactions on Electron Devices, 2019, 66, 1396-1401.	3.0	2
56	A simplified adaptive sparse digital preâ€distorter for joint mitigation of frequencyâ€dependent transmitter impairments. International Journal of RF and Microwave Computer-Aided Engineering, 2020, 30, e22056.	1.2	2
57	Low-firing behavior, microstructure, and electromagnetic properties of a ferroelectric-ferromagnetic composite material with multiple doping. Journal of Alloys and Compounds, 2018, 750, 479-489.	5.5	1
58	Power Amplifier Behavioral Model Dimension Pruning Using Sparse Principal Component Analysis. , 2018, , .		1
59	Synthesizing and Optimizing of Wide Stopband Low-Pass Filter with Improved Infinite Attenuation Unit Based on Stubs. Frequenz, 2018, 72, 523-531.	0.9	1
60	SIWâ€based microfluidically tunable PD with wideâ€frequencyâ€ŧuning range. Electronics Letters, 2019, 55, 40-41.	1.0	1
61	Design of Duplex Terahertz Waveguide Rotary Joint Based on Septum Polarizer. , 2021, , .		1
62	A Room Temperature Polymer-Coated Piezoresistive Silicon Bridge Gasoline Vapor Sensor. IEEE Sensors Journal, 2012, 12, 926-929.	4.7	0
63	A novel design method for extending power backâ€off range of broadband Doherty power amplifier. Microwave and Optical Technology Letters, 2019, 61, 2420-2426.	1.4	0
64	An accurate continuous-time model for current-mode boost convertors which integrates the current-loop instability scheme. , 2014, , .		0
65	Design of a Phased Array Fed Reflector Antenna for Limited Scanning. , 2021, , .		0